Virtual Model Control for Dynamic Banlance of a Two Wheeled-legged Robot

Xiaopeng Huang
State Key Laboratory of Fluid Power and Mechatronic Systems, School of Mechanical Engineering, Zhejiang University, Hangzhou 310027, China
xphuang@zju.edu.cn

Tao Liu*
State Key Laboratory of Fluid Power and Mechatronic Systems, School of Mechanical Engineering, Zhejiang University, Hangzhou 310027, China
liutao@zju.edu.cn

Meimei Han
Zhejiang Fuzhi Science and Technology Innovation Co., Ltd.
Hangzhou 310027, China
mmhan@zju.edu.cn

João P. Ferreira
Institute of Superior of Engineering of Coimbra
Quinta da Nora
3030-199 Coimbra, Portugal
ferreira@mail.isec.pt

***Abstract*—Wheeled-legged robot integrates the strong points of the legged and wheeled robot, it has the characteristics of flexible movement and strong anti-interference ability, which make it have great potential in survey, indoor service and disaster rescue scenarios. This paper design the mechanical structure, and then derive a three-dimensional dynamic model of the robot. Next, linear quadratic regulator(LQR) methods are designed to keep the balance of the robot, and the virtual model control (VMC) method is exploited to control the leg. The simulation and experimental results show that the designed linear quadratic regulator can keep the balance of the robot, while the VMC method can achieve the changes in leg posture of the robot.**

Keywords—wheeled-legged robot, under-actuated robotics optimization, modeling,

I. INTRODUCTION

With the rapid development of technology, robots are starting to replace humans in various fields such as production, health care, service and space[1]. In the research of robots, the mobility ability is the most critical part of the robot, which determines the scene of the robot's work and its efficiency. At present, land robots are mainly include wheeled robots and legged robots. The wheeled robot has the advantage of fast moving speed, but their poor adaptability makes them more difficult to cope with complex terrain. The legged robot has become the object of research by its super adaptability to the ground. Its rich movement forms allow it to cope with complex scenes easily, but its movement efficiency is not high enough.

In order to solve the problem of adaptability and movement ability, wheel-legged robot came into being. By adding wheels at the end of the leg of legged robot, it has the advantages of high mobility efficiency of wheeled robot and can deal with complex terrain[2]. In the future, with the help of artificial intelligence technology, wheel-legged robots will have a wide range of application scenarios and markets[3].

The adaptability and maneuverability of wheel-legged robot have high research value. As early as 1998, Professor Osamu Matsumot and others from Gifu University in Japan developed a 5-DOF "bipedal type - bipedal robot"[4]. Wheel-legged robots have developed rapidly in the past few decades. The Handle, released by Boston Dynamics, can handle tasks such as carrying items and unloading cargo on its own while maintaining balance[5]. Ascent of Eidgenössische Technische Hochschule Zürich designed the leg three-link scheme and proposed a whole body control scheme with model-based linear quadratic regulator assistance to improve the stability and robustness of the robot[6]. Tencent's Ollie adds a balance leg to the wheel-legged robot to provide extra angular momentum for the robot, and directly proposes the method of applying the interconnection and damping assignment - passivity-based control (IDA-PBC) to the nonlinear dynamic model of the robot to balance the robot [7].

At present, most of the research on wheel-legged robot is simplified as a wheel inverted pendulum(WIP) model, and the longitudinal balance is mainly studied. This has the advantage of reducing the model to a plane with the dynamics of an inverted pendulum. However, it ignores the lateral motion of the pendulum and thus the component of the centrifugal force[8]. In this paper, a new dynamic model is used, which considers not only the longitudinal equilibrium, but also the rotational motion of the pendulum.

On the basis of the dynamic model, this paper uses LQR-assisted control to achieved the stability and drive of the system[9], and adopts the method of VMC in the leg control. For the sake of verify the feasibility of the algorithm, some experiments are put into practice on the actual equipment designed. Using this dynamic model, it is unnecessary to design a new controller for steering motion

The section II introduces the mechanical structure of the robot and the hardware design of the wheeled-legged robot experimental platform. In section III, a new three-dimensional model is presented, and the kinematic model and dynamic model are analyzed. Section IV mainly introduces the control system of the system, including the balance control of Section IV-A and leg control of IV-B. The simulation which carried out in Matlab and Simulink environment and true world experiments are proposed in section V. Finally, the conclusion will be in Section VI.

II. SYSTEM DESCRIPTION

A. Mechanical Design

The wheel-legged robot platform is shown in Figure 1 .It is composed of a main body and two legs with wheels at the end of the legs. Compared with the traditional three bar linkage mechanism, the four bar linkage mechanism with

2022 International Conference on Service Robotics (ICoSR) | 978-1-6654-5438-4/22/$31.00 ©2022 IEEE | DOI: 10.1109/ICOSR57188.2022.00016

978-1-6654-5438-4/22/$31.00 ©2022 IEEE
DOI 10.1109/ICoSR57188.2022.00016

planar parallel connection is used in the mechanical mechanism, which provides more force and has a more compact structure[7]. The legs are connected to the body of the robot, and the upper part of the body houses the microcontroller, actuator and other electrical equipment. The leg mechanism has five independently retractable rotary joints. The robot moves as shown in Figure 1(a) and moves freely at high speed with a low center of gravity. When complex movements are required, the leg length changes into the standing posture shown in Figure 1(b).

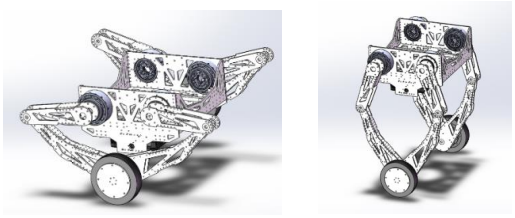

(a) Ordinary posture (b) Standing posture

Fig. 1: Wheel-legged robot prototype designed in this paper

B. Hardware

How to select the most suitable electromechanical system is a complex and difficult process. To ensure that the robot can perform stable jumps, the torque of the joint motor needs to be high enough. For this purpose, the Unitree A1 motor provides torque of up to 33.5NM and has built-in sensors to provide perceptual feedback. The hub motor uses K-TECH's MF9025 motor with a maximum torque of 4.5NM. Each motor has a built-in encoder that provides precise speed and position information. The joint motor communicates using the Controller Area Network, and the joint motor communicates with the microcontroller via RS-485 serial to USART. The system is also uses an IMU to measure the attitude and a time-of-flight (ToF) distance sensor to measure the altitude above the ground. The system is powered by 24V lithium battery. The actual measurement shows that the weight is about 9.25kg and the running time is about 2.5 hours. Table I show the robotic electrical equipment list.

C. Software

In the design of the algorithm, some complex matrix operations do not need real-time calculation, can be carried out in advance, so the requirements for the controller is not so high, can use microcontroller as a controller. ST's STM32 series of high performance processors has been able to meet demand. Code is divided into perception, decision, and control layers. The perception layer obtains the sensor data of inertial measurement unit(IMU) and motor encoder, and a Kalman filter is implemented on them. On this basis, a observer is designed to estimate the state of the system. The decision layer sends the data processed by the perception layer to the controller together with the user's expectation data. The leg control and balance control are decoupled in the design, so the controller can be independent. User input comes from the remote control or the keyboard and mouse on the PC. According to the actual model, the control layer fuses the output torque of the decision layer and sends the driving signal to each motor.

TABLE I. ROBOTIC ELECTRICAL EQUIPMENT

Component	Name
Microcontroller	STM32F407VET6
Wheel Motor	K-TECH MF9025 * 2
Joint Motor	Unitree A1 * 4
Joint Motor 485-to-USART	MCS-52A
Battery	DJI TB48S
IMU	BMI088
Remote Controller	DJI DT7

III. DYNAMIC MODEL

The correct modeling of the mechanical structure of the robot can better understand and analyze the physical properties of the system and design a reasonable control algorithm.

A. Kinematical modeling

To simplify the model of the wheel-legged robot, we can reduce it to a system as shown in Figure 2, which consists of two parts, the wheels and an inverted pendulum on a cart in the middle. Table 2 lists the main model parameters of the system.

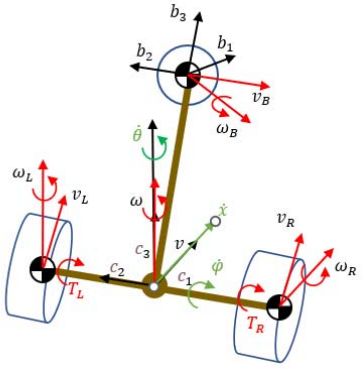

Fig. 2. 3D Schematic Diagram of Wheel Inverted Pendulum Model.

TABLE II. DEFINED MODEL PARAMETERS

Symbol	Definition
r, d, l	Radius of wheels, Distance among the two wheels, Height of center of mass,
m_B, m_W	Weight of the inverted pendulum body (excluding wheels), Weight of wheel
v_L, v_R, v_B	Velocities of the centers of mass of left wheels, right wheels and body
$\omega_L, \omega_R, \omega_B$	Angular velocities of left wheels, right wheels and body
T_L, T_R	Wheel torque for left and right wheels
f_L, f_R	Damping torques generated at left and right wheels
$\dot{x}, \dot{\phi}, \dot{\theta}$	Forward velocity, pitch rate, yaw rate
I_o, I_{oxy}	Mass moment of inertia of wheel with respect to the wheel axis and the radial axis
I_1, I_2, I_3	MOI of the pendulum body with respect to xyz axis

From Figure 2 we can obtain that the coordinates of each center of mass have the following constraints:

$$x_B = x_C + l\sin\varphi\cos\theta\ , y_B = y_C + l\sin\varphi\sin\theta$$

$$z_B = l\cos\varphi$$

$$x_L = x_C - (d/2)\sin\theta\ , y_L = y_c + (d/2)\cos\theta \qquad (1)$$

$$x_R = x_C + (d/2)\sin\theta\ , y_R = y_c - (d/2)\cos\theta$$

The direction of the motion of the robot cannot be perpendicular to the rolling direction of the wheel, that is, the robot has no side sliding, so a constraint equation can be obtained. In addition, the motion generated by the robot can only be generated by the rolling of the left and right wheels. Two other constraint equations are obtained:

$$\dot{x}\sin\theta - \dot{y}\cos\theta = 0$$

$$\dot{x}\cos\theta + \dot{y}\sin\theta + \frac{d}{2}\dot{\theta} - r\dot{\theta}_r = 0 \qquad (2)$$

$$\dot{x}\cos\theta + \dot{y}\sin\theta - \frac{d}{2}\dot{\theta} - r\dot{\theta}_r = 0$$

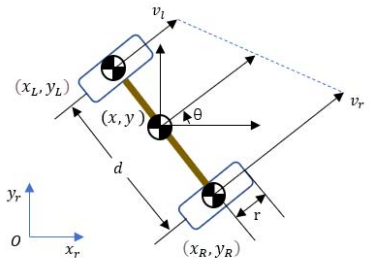

Fig. 3. Top view of wheel inverted pendulum model.

Considering that for the whole system framework, the palstance of the three objects can be represented as

$$\omega_L = \dot{\theta}c_3 + (1/r)(\dot{x} - d\dot{\theta}\ /\ 2)c_2$$

$$\omega_R = \dot{\theta}c_3 + (1/r)\big(\dot{x} + d\dot{\theta}/2\big)c_2 \qquad (3)$$

$$\omega_B = (-\dot{\theta}\sin\varphi)b_1 + \dot{\varphi}b_2 + (\dot{\theta}\cos\varphi)b_3$$

Similarly, the linear velocity can be expressed as

$$v_L = \dot{x}c_1 + \omega_c(d\ /\ 2)c_2 = (\dot{x} - d\dot{\theta}\ /\ 2)c_1$$

$$v_R = \dot{x}c_1 + \omega_c(-d/2)c_2 = \big(\dot{x} + d\dot{\theta}/2\big)c_1 \qquad (4)$$

$$v_B = \dot{x}c_1 + \omega_B l b_3 = \dot{x}c_1 + (l\dot{\varphi})b_1 + (l\dot{\theta}\sin\varphi)\,c_1$$

B. Dynamics modeling

In general, there are two approaches to deriving dynamical models: the Euler-Lagrange method and the recursive Newton-Euler method. The former considers the whole system as a whole, and uses Lagrange function (the difference between kinetic energy and potential energy of mobile robot) to analyze the dynamic model. The latter uses a recursive approach, considering the relationship between the forces of each link to arrive at the final model. Compared with Newton-Euler method, Lagrangian method does not depend on the spatial coordinate system, and does not need to analyze the internal constraints of the system. In this paper, the Euler-Lagrange method is used to analyze the dynamics of a wheeled inverted pendulum model.

$$x_R = x_C + (d/2)\sin\theta\ , y_R = y_c - (d/2)\cos\theta \qquad (5)$$

Lagrange equation is expressed as

$$\frac{d}{dt}\left(\frac{\partial L}{\partial \dot{q}_i}\right) - \frac{\partial L}{\partial q_i} = Q_i \qquad i = 1, \ldots, n \qquad (6)$$

where q_i is the generalized coordinate, and Q_i is the generalized force of the corresponding coordinate, and L is the Lagrangian function, and it can be expressd as:

$$L = T - V \qquad (7)$$

Where K is the total kinetic energy and P is the potential energy of the system.

Therefore, we can get the translational kinetic energy of the wheel-legged robot in Figure 1 can be related to:

$$T_{trans} = \frac{1}{2}m_W(v_L \cdot v_L) + \frac{1}{2}m_W(v_R \cdot v_R) + \frac{1}{2}m_B(v_B \cdot v_B) \qquad (8)$$

According to the MOI , the rotational kinetic energy can be written as:

$$T_{rot} = \frac{1}{2}(\omega_L)^T I_L \omega_L + \frac{1}{2}(\omega_R)^T I_R \omega_R + \frac{1}{2}(\omega_B)^T I_B \omega_B \qquad (9)$$

The body of the wheeled legged robot in this paper is symmetric, so the inertia matrix has the diagonal form

$$I_L = I_R = diag\{I_{oxy}, I_o, I_{oxy}\}, I_B = \mathrm{diag}\{I_1, I_2, I_3\} \qquad (10)$$

The direction of the instantaneous motion of the robot

When the wheel-legged robot moves on a flat surface, the vertical motion occurs only through the inverted pendulum. Thus, the potential energy is

$$V = m_B g l\cos\varphi \qquad (11)$$

After obtaining the above equations, it can be expressed into the Lagrange function of the system. Our generalized coordinates, $q = [x, \theta, \varphi]$, are chosen to represent the forward position of the robot, the orientation Angle and the tilt Angle of the inverted pendulum, so that $\dot{q} = [v, \omega, \dot{\varphi}]$. After derivation, simplification, and translation into matrix form, we can get

$$M(q)\ddot{q} + C(q, \dot{q})\dot{q} + D\dot{q} + G(q) = Bu \qquad (12)$$

where

$$M = \begin{bmatrix} a_{11} & a_{12} & 0 \\ a_{21} & a_{22} & 0 \\ 0 & 0 & a_{33} \end{bmatrix}, C = \begin{bmatrix} 0 & c_{12} & c_{13} \\ 0 & 0 & c_{23} \\ c_{31} & c_{32} & c_{33} \end{bmatrix}, q = \begin{bmatrix} x \\ \varphi \\ \theta \end{bmatrix},$$

$$D = \begin{bmatrix} d_{11} & d_{12} & 0 \\ d_{21} & d_{22} & 0 \\ 0 & 0 & d_{33} \end{bmatrix}, B = \begin{bmatrix} b_{11} & b_{12} \\ b_{21} & b_{22} \\ b_{31} & b_{32} \end{bmatrix},$$

$$u = \begin{bmatrix} T_L \\ T_R \end{bmatrix}, G = [0, -m_B lgsin\varphi, 0]^T$$

$a_{11} = m_B + 2m_w + 2I_o/r^2, a_{12} = a_{12} = m_B lcos\varphi,$

$a_{22} = I_2 + m_B l^2,$

$a_{33} = I_3 + 2I_{oxy} + \frac{(m_w + I_o/r^2)d^2}{2} - (I_3 - I_1 - m_B l^2)\sin^2\varphi,$

$b_{11} = b_{12} = 1/r, b_{21} = b_{22} = -1,$

$b_{31} = -d/2r, b_{32} = d/2r,$

$c_{12} = -m_B l\dot{\varphi} sin\varphi, c_{13} = -m_B l\dot{\theta} sin\varphi,$

$c_{23} = (I_3 - I_1 - \dot{m}_B l^2)\dot{\theta} sin\varphi cos\varphi, c_{31} = m_B l\dot{\theta} sin\varphi,$

$c_{32} = -(I_3 - I_1 - m_B l^2)\dot{\theta} sin\varphi cos\varphi,$

$c_{33} = -(I_3 - I_1 - m_B l^2)\dot{\varphi} sin\varphi cos\varphi,$

$d_{11} = 2c_a / r^2, d_{12} = d_{21} = -2c_a / r,$

$d_{22} = 2c_a, d_{33} = (d^2/2r^2)c_a$

C. Linearization

The trajectory of the phase diagram of the nonlinear system in a small area of equilibrium is close to that of the linearized system. Selecting a state variable

$$\xi = \left[\dot{x}, \dot{\theta}, \dot{\varphi}, x, \theta, \varphi\right]^T, u = [T_L, T_R]^T, \dot{\xi} = f(\xi, u) \quad (13)$$

When $\dot{\xi} = f(\xi, u) = 0$, there's an equilibrium point $\xi_0 = \left[\dot{x}, \dot{\theta}, \dot{\varphi}, x, \theta, \varphi\right]^T = [0,0,0,0,0,0]^T$, the robot remains upright with zero forward and angular velocity. Compute the linearized state space matrix.

$$A = \frac{\partial f}{\partial \xi}, \qquad B = \frac{\partial f}{\partial u} \quad (14)$$

After taking the partial derivative of the nonlinear system equation, the linearized model can be obtained

$$\dot{\xi} = A\xi + Bu \quad (15)$$

D. Leg Modeling

In order to obtain the leg length L of the robot, it is essential to solve the forward kinematics of the robot. The schematic diagram of the planar five-link mechanism of the robot leg is shown in Figure 4.

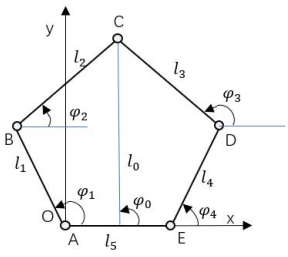

Fig. 4. Schematic diagram of planar five bar linkage

Taking point A as the origin of the coordinate system, we can obtain the position equation of point C as

$$x_C = x_B + l_2\cos\varphi_2 = x_D + l_3\cos\varphi_3$$

$$y_C = y_B + l_2\sin\varphi_2 = y_D + l_3\sin\varphi_3 \quad (16)$$

$$x_B = x_A + l_1\cos\varphi_1,\ y_B = y_A + l_1\sin\varphi_1$$

Solving the system of equations can obtain

$$\varphi_2 = 2\arctan\left(\frac{B_0 + \sqrt{A_0^2 + B_0^2 - C_0^2}}{A_0 + C_0}\right) \quad (17)$$

where $A_0 = 2l_2(x_D - x_B)$, $B_0 = 2l_2(y_D - y_B)$, $C_0 = l_2^2 + l_{BD}^2 - l_3^2$, $l_{BD} = \sqrt{(x_D - x_B)^2 + (y_D - y_B)^2}$, in the same way, we can get φ_3.

By solving the above system, the coordinates of C can be found, the same to l_0 and φ_0.

IV. CONTROL STRATEGY

Through the analysis, we can get that the wheel-legged robot is an unstable under-actuated system. Since balance control and leg control are decoupled, we can control them independently.

A. balance Control

According to the state space equation obtained in Section III, we transform the system into a linear system. Assuming that the system is in a stable state, the control law of the robot can be assumed to be:

$$u = -K\tilde{\xi} \quad (18)$$

where K is the gain matrix and $\tilde{\xi}$ is provided by the state observer with a Kalman filter. The used approach is LQR control method. LQR is used to solve the linear quadratic problem to obtain the optimal control quantity. Define the cost function J as:

$$J = \int_0^\infty (\xi^T Q\xi + u^T Ru)\,dt = \int_0^\infty \xi^T (Q + K^T RK)\xi^T\,dt \quad (19)$$

To minimize J, then the gain matrix K needs to satisfy:

$$K = R^{-1}B^T P \quad (20)$$

where P is a positive definite constant matrix and satisfies the following Riccati algebraic equation :

$$PA + A^T P - PBR^{-1}B^T P + C^T QC = 0 \quad (21)$$

At this point, the LQR method is completed, where Q and R matrices are positive semidefinite state weighting matrices and positive definite control weighting matrices, respectively. The parameter Settings are given by the designer and affect the speed of state variable adjustment and the size of system control input. It needs to be adjusted according to actual application scenarios.

B. Leg Control

Virtual model control(VMC) is a force control algorithm, which comprehensively considers the position, speed and attitude of the robot control, through the adjustment of parameters, the position and attitude of the comprehensive tracking[10]. At each degree of freedom to be controlled, an imaginary spring damping component is constructed to link the internal operating point of the robot with its external dot[11]. The virtual force is transformed by the action of the actuator, and the virtual force between the connection points is used to guide the robot to achieve the target motion. In order to obtain the desired joint torque through the virtual force, it is essential to convert the force in the global space into the joint torque, that is, the forward motion model:

$$x = f(q) \tag{22}$$

where $x = [L_0, \varphi_0]^T$, $q = [\varphi_1, \varphi_4]^T$

Take the partial of x with respect to q can get jacobian matrix J, thus

$$\delta x = J\delta q \tag{23}$$

The Jacobian matrix J can be used to map the joint velocity into the attitude change rate. According to the virtual work theorem, we have

$$T^T\delta q + (-F)^T\delta x = 0 \tag{23}$$

where T is the torque of each joint, F is the virtual force, and Equation (23) can be expressed as

$$T = J^T F \tag{24}$$

The virtual component composed of spring and damper can ensure certain extension and stability, and the virtual force can be expressed as

$$F = K_P(P - P_d) + K_d(V - V_d) \tag{25}$$

where K_P and K_D are elastic coefficient matrix and damping coefficient matrix, P and V are the actual position and velocity, P_d and V_d are the expected position and velocity.

V. Simulations and Experiments

robot is an unstable under-actuated system. Since balance control and leg control are decoupled, we can control them independently.

A. Simulations

All control algorithms are tested in MATLAB/Simulink. In the simulation environment, the actual robot model is imported, and the system state is tested according to the changing trend in the actual environment. It provides the basis for real machine experiment. Specifically, the following cases are designed.

*1) Starting Up :*The simulation experiments of the robot from the initial attitude to the balance attitude are carried out. Assume that the initial Angle of the robot is 35 degrees, and the result is shown in Figure 5. In Figure 5(a), the red solid line is the real Angle, and the blue dashed line is the target Angle.

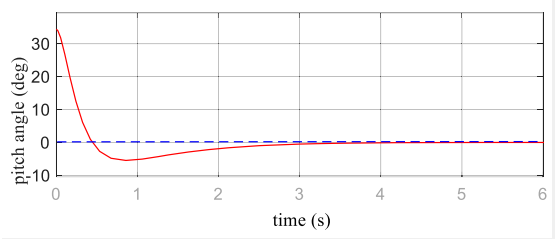

(a) Pitch angle φ

*2) Changing Height:*While standing at balance, change the target height. The height of the target is set as 20cm, and the virtual force and left and right torque are shown in Figure 6

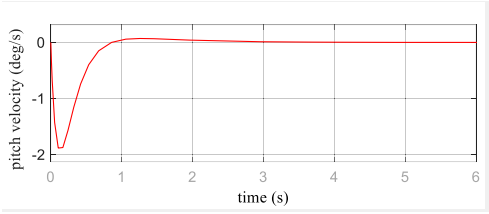

(b) Pitch velocity $\dot{\varphi}$

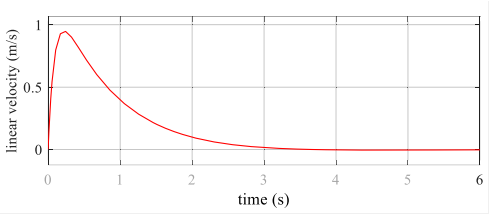

(c) Linear velocity $\dot{x}$

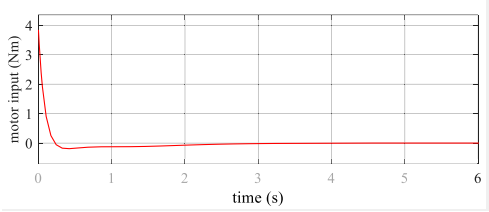

(d) Motor input τ

Fig. 5 Simulation results of starting up

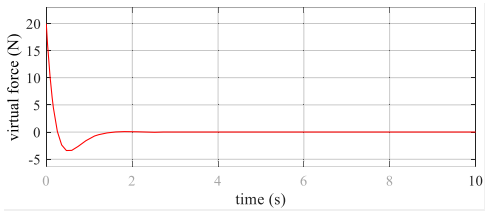

(a) virtual force F

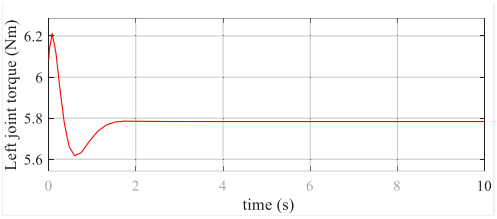

(b) Left joint motor input τ_l

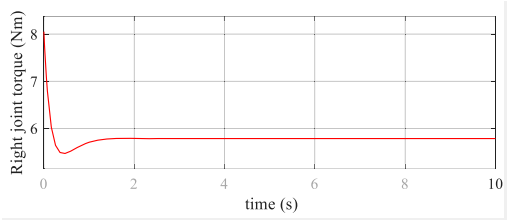

(c) Right joint motor input τ_r

Fig. 6 Simulation results of changing height

B. *Experiments*

In the actual experiment, the following two cases are considered:

1) Starting Up: As shown in Figure 7(a), the offset Angle of the robot is 36° in the initial condition, and Figure 8 shows that the robot can quickly reach the balance.

2) Changing Height: The standing posture of the robot is indicated in Figure 7(b) and Figure 7(c). The robot can adjust its posture by changing the height of the body through the joint motor. The torque of the four articulated motors is indicated in Figure 9.

(a) Initial condition (b) Standing still

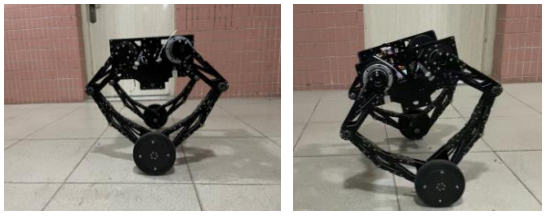

(c) Changing height (d) Moving

Fig. 7 The balance experiments

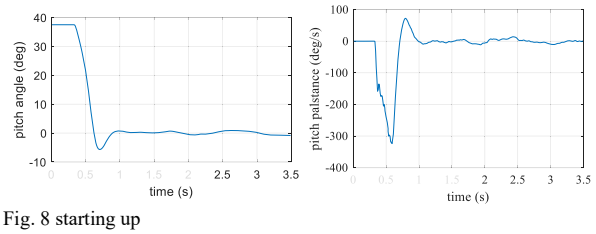

Fig. 8 starting up

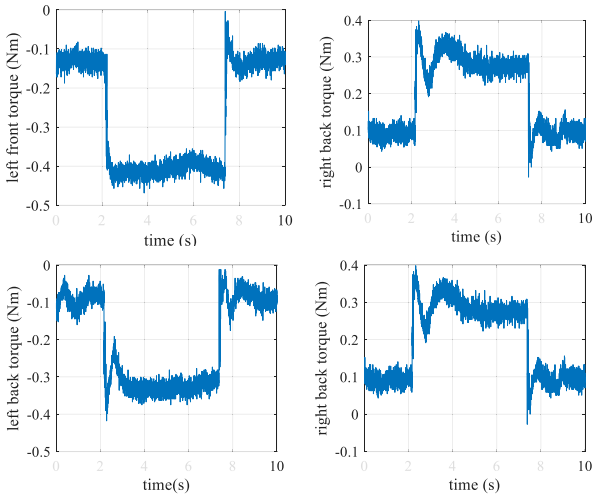

Fig. 9 Simulation results of starting up

The experimental results verify the feasibility of the algorithm, and show that the robot has good stability and response speed. We will investigate more advanced control strategies in future work.

VI. Conclusion

In this paper, a new wheel-legged robot is introduced, and a new 3-DOF dynamic modeling model is used. The LQR control method combined with sensor data was used to keep the balance of the robot, and the VMC method was used to control the leg motion of the robot. Simulation and experiment show that the algorithm is feasible and has good anti-interference ability.

Acknowledgment

This work was supported in part by the Natural Science Foundation of Zhejiang under awards LZ20E050002, the Key Research and Development Program of Zhejiang under awards 2022C03103 and 2021C030051, and Open Fund of the State Key Laboratory of Fluid Power and Mechatronic Systems: GZKF-202101.

References

[1] R. Siegwart and I. R. Nourbakhsh, Autonomous Mobile Robots. The MIT Press Cambridge, Massachusetts, 2004.

[2] M. Hutter, C. Gehring, A. Lauber, F. Gunther, C. D. Bellicoso, V . Tsounis, P . Fankhauser, R. Diethelm, S. Bachmann, M. Blösch et al., “Anymal-toward legged robots for harsh environments,” Advanced Robotics, vol. 31, no. 17, pp. 918–931, 2017.

[3] J. Chestnutt, P . Michel, J. Kuffner and T. Kanade, Locomotion among dynamic obstacles for the honda ASIMO, in Proceedings of IEEE/RSJ International Conference on Intelligent Robots and Systems, 2007: 2572-2573.

[4] Matsumoto O, Kajita S, Saigo M, et al. Dynamic Trajectory Control of Passing over Stairs by a Biped Type Leg-wheeled Robot with Nominal Reference of Static Gait[J]. Journal of the Robotics Society of Japan, 1998, 16(6): 868-875.

[5] Handle. Accessed: 29.07.2018. [Online]. Available: https://www.bostondynamics.com/handle

[6] V. Klemm et al., "Ascento: A Two-Wheeled Jumping Robot," 2019 International Conference on Robotics and Automation (ICRA), 2019, pp. 7515-7521, doi: 10.1109/ICRA.2019.8793792.

[7] Wang S, Cui L, Zhang J, et al. Balance control of a novel wheel-legged robot: Design and experiments[C]//2021 IEEE International Conference on Robotics and Automation (ICRA). IEEE, 2021: 6782-6788.

[8] S. Kim and S. Kwon, “Dynamic modeling of a two-wheeled inverted pendulum balancing mobile robot,” International Journal of Control, Automation and Systems, vol. 13, no. 4, pp. 926–933, 2015.

[9] K. Victor, M. Alessandro, G. Lionel, M. Dominik, R. David, K. Mina, D. Yvain and S. Roland, LQR-assisted whole-Body control of a wheeled bipedal robot with kinematic loops, IEEE Robotics and Automation Letters, 5(2) 3745-3752.

[10] Raibert Marc H.. Trotting, pacing and bounding by a quadruped robot[J]. Journal of Biomechanics, 1990, 23 : 79-98.

[11] Huixiang Xie et al. An intuitive approach for quadruped robot trotting based on virtual model control[J]. Proceedings of the Institution of Mechanical Engineers, Part I: Journal of Systems and Control Engineering, 2015, 229(4) : 342-355.